Journal of the European Ceramic Society **6** (1990) 119–127

Sialon Ceramics Made with Mixtures of Y_2O_3–Nd_2O_3 as Sintering Aids

Per-Olov Käll & Thommy Ekström

Department of Inorganic Chemistry, Arrhenius Laboratory, University of Stockholm, S-106 91 Stockholm, Sweden

(Received 18 December 1989; revised version received 2 March 1990; accepted 15 March 1990)

Abstract

Sialon ceramics have been prepared by pressureless sintering at 1775 and 1825°C, using mixtures of Y_2O_3–Nd_2O_3 as sintering aids. It was found that at 1775°C less dense materials were obtained, but by raising the sintering temperature to 1825°C fully dense materials could be produced, even when pure neodymia was used. The hardness of the Nd-sialon ceramics was found to be slightly lower than for the corresponding Y-sialon ceramics, but the fracture toughness was approximately the same. It was also observed that the amount of intergranular phase increased when yttria was replaced by neodymia.

Sialon-keramische Werkstoffe wurden durch druckloses Sintern bei 1775 und 1825°C unter Zusatz von Y_2O_3–Nd_2O_3 als Sinterhilfsmittel hergestellt. Bei einer Temperatur von 1775°C konnten nur Materialien mit geringerer Dichte erzielt werden doch durch die Erhöhung der Sintertemperatur auf 1825°C konnten, selbst bei ausschließlicher Verwendung von Neodymoxid, völlig dichte Proben erhalten werden. Die Härte der Nd-sialon Werkstoffe lag etwas niedriger als für die entsprechenden Y-sialon Werkstoffe, die Bruchzähigkeit war jedoch näherungsweise gleich. Es wurde ferner beobachtet, daß der Ersatz von Y_2O_3 durch Nd_2O_3 den Anteil an Korngrenzenphase erhöhte.

On a préparé des sialons par frittage naturel à 1775 et 1825°C, en utilisant des mélanges Y_2O_3–Nd_2O_3 comme additifs. La température de 1825°C s'est avérée nécessaire pour une densification complète des matériaux; celle-ci a été observée même pour l'oxyde de néodyme pur. La dureté du Nd-sialon est légèrement inférieure à celle du Y-sialon correspondant, alors que leur ténacité est quasiment la même. La quantité de phase intergranulaire augmente lorsque l'on remplace l'yttrine par l'oxyde de néodyme.

1 Introduction

It is well known that the covalent nature of the bonds in the Si_3N_4 structure gives rise to very low self-diffusion rates even at high temperatures close to decomposition. This explains why Si_3N_4 cannot be densified by pressureless sintering without a considerable amount of sintering additives, which allow densification through a liquid phase. The silicon nitride dissolves in the formed liquid and, as both aluminium and oxygen are present in the melt, α and/or β sialon crystals precipitate according to the overall composition in the M–Si–Al–O–N phase diagram (Fig. 1a). The β sialon $Si_{6-z}Al_zO_zN_{8-z}$, with $0 \leq z \leq 4$, has a linear extension in the phase diagram, whereas the α sialon solid solution is represented by a two-dimensional area, $M_xSi_{12-(m+n)}Al_{m+n}O_nN_{16-n}$, with $x < 2$ (when M is

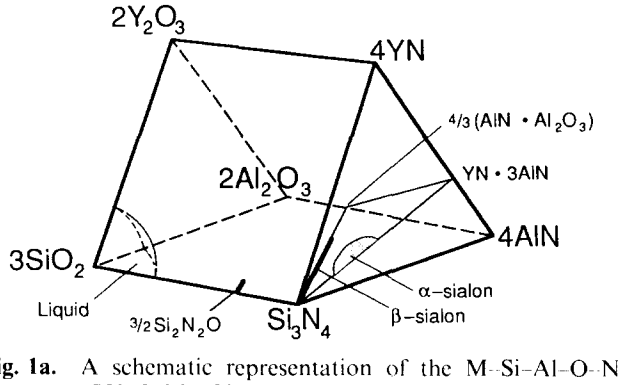

Fig. 1a. A schematic representation of the M–Si–Al–O–N system at 1750 C (M = Y or Nd). The β sialon, $Si_{6-z}Al_zO_zN_{8-z}$, with $z \leq 4$, has a linear extension in the base plane of the Jänecke prism. The α sialon solid solution, $M_x(Si, Al)_{12}(O, N)_{16}$, has a two-dimensional extension in a plane defined by the three corners Si_3N_4–$(4/3)Al_2O_3 \cdot AlN$–$MN \cdot 3AlN$.

Journal of the European Ceramic Society 0955-2219/90/$3.50

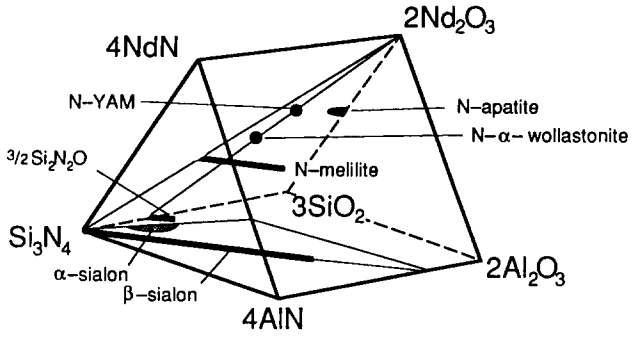

Fig. 1b. The Nd–Si–Al–O–N system. The Nd-melilite phase has a linear extension according to the formula $Nd_2Si_{3-x}Al_xO_{3+x}N_{4-x}$ with $x \leq 1$.

a trivalent cation, $x = m/3$). The α sialons thus need a stabilizing cation of suitable size, and both Y^{3+} and Nd^{3+} belong to this group.[1]

Yttria is still by far the most important sintering aid for silicon nitride ceramics, but neodymia has been mentioned as a possible candidate to replace yttria because of its lower price. The phase relationships in the Nd–Al–O–N and the Nd–Si–Al–O–N systems have been thoroughly studied by Slasor *et al.*[2] They found an extended liquid-phase region at high temperatures and observed that the refractory phases formed in the Nd-containing systems in most cases are analogous to those observed in the corresponding Y-systems. However, one notable difference is that the melilite phase ($M_2O_3.Si_3N_4$) is considerably more extended along the tie-line $M_2Si_3O_3N_4$–$M_2Si_2AlO_4N_3$ in the Nd-system than in the Y-system (Fig. 1b).

With this background, pressureless sintering of Nd-sialon ceramics seems feasible, and the eutectic temperatures in the Nd-systems are generally somewhat lower than those in the Y-sialon system. However, it has been suggested that formation of substantial quantities of Nd-melilite, especially if it occurs in the early stages of the sintering cycle, may prevent good densification and lower the degree of conversion of the silicon nitride to the sialon phases. More particularly, the formation of α sialon might be blocked. In an earlier paper[3] we have reported the sintering behaviour when Nd_2O_3 is substituted for Y_2O_3 in pressureless sintering of sialon materials at 1775°C. In this paper, we are dealing with the behaviour when the sintering temperature is raised to 1825°C.

2 Experimental

The materials were prepared in 500-g batches, and the overall composition of the materials selected for this study are given in Fig. 2. Equivalents in the three-dimensional M–Si–Al–O–N Jänecke prism (M = Y or Nd) are defined according to the formulae

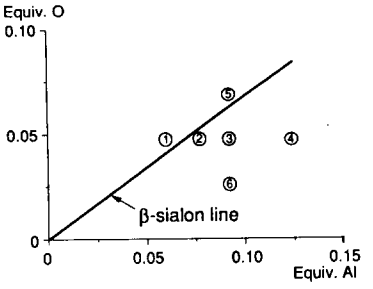

Fig. 2. The overall composition of the samples selected for this study, when the oxygen present in the Y_2O_3 and Nd_2O_3 additives has not been included in the calculation of the oxygen equivalents. However, if the oxygen in the additives is included, one has to add about 0·018 O-equivalents to all compositions. The Al-equivalents, on the other hand, will be only slightly decreased due to the presence of Y and Nd, and the shift will be hardly observable on this scale.

$$Al_{eq} = 3Al_{at}/(3Al_{at} + 3M_{at} + 4Si_{at})$$
$$M_{eq} = 3M_{at}/(3Al_{at} + 3M_{at} + 4Si_{at})$$
$$Si_{eq} = 1 - Al_{eq} - M_{eq}$$
$$O_{eq} = 2O_{at}/(2O_{at} + 3N_{at})$$
$$N_{eq} = 1 - O_{eq}$$

where the indices 'eq' and 'at' denote equivalents and atomic fractions respectively. Using these expressions it can be shown that any point in the Jänecke prism can be described by the formula

$$Si_{3(1-Al_{eq}-M_{eq})}Al_{4Al_{eq}}M_{4M_{eq}}O_{6O_{eq}}N_{4(1-O_{eq})}$$

with

$$0 \leq 1-Al_{eq}-M_{eq} \leq 1$$

The same constant molar amount of Y_2O_3/Nd_2O_3 was added to all samples, corresponding to 6·0 wt% for the pure yttria and 8·9 wt% for the pure neodymia materials. Each of the samples shown in Fig. 2 was prepared in three compositions, where the Y_2O_3/Nd_2O_3 molar ratio was varied as 100/0, 50/50 and 0/100. For sample 3 the intermediate mixtures 75/25 and 25/75 were also prepared.

The green powder mixtures were prepared using Si_3N_4 (H.C. Starck-Berlin, LC1), Al_2O_3 (Alcoa, A16SG), AlN (H.C. Starck-Berlin, grade A), Y_2O_3 (99·9%, H.C. Starck-Berlin) and Nd_2O_3 (>99·5%, Molycorp. Inc). The yttria and neodymia materials were calcined at 1000°C for 2 h before use.

In the preparations of the samples, corrections were made for the small amounts of oxygen present as oxides or oxynitrides in the Si_3N_4 and AlN raw materials. The analyzed oxygen content of the silicon nitride material corresponded to 2·9 wt% SiO_2 and of the aluminium nitride material to

1·9 wt% Al_2O_3. The starting materials were mixed in water-free propanol and ground in a vibratory mill for 16 h with sialon milling media. The slurry was dried, and powder compacts of grain size 16 mm × 16 mm × 6 mm were pressed at 125-MPa load. Before firing, the specimens were embedded in micron-sized boron nitride powder in graphite crucibles. The sintering was performed in a production furnace of 240 dm^3 volume at 1775 or 1825°C for 2 h in nitrogen gas at atmospheric pressure, to simulate the heating/cooling rates in a furnace of high thermal mass. The heating rate to the soaking temperature was 650°C/h in the 'low' temperature range and 100°C/h for the last 50°C to approach the final temperature smoothly. The cooling rate for the first 300°C from the sintering temperature was about 500°C/h.

The densities of the sintered specimens were measured by Archimedes' principle in a toluene bath with an accuracy of 0·002 g cm^{-3}. Before physical characterization the specimens were ground and polished according to standard techniques. Hardness (HV10) and indentation fracture toughness (K_{IC}) at room temperature were obtained by a Vickers diamond indenter with a 98-N (10-kg) load, and the fracture toughness was evaluated according to the method of Anstis *et al.*,[4] assuming a value of 300 GPa for Young's modulus.

X-Ray diffraction analysis was performed both by diffractometer (Rigaku with rotating Cu-anode ~10 kW output power) on a selected number of specimens with polished surfaces and by the Guinier–Hägg film technique on all samples, using a slice of sintered material crushed to powder and with silicon as an internal standard. The lattice parameters of the different phases were refined with a least-squares program. The z-value of the β-sialon phase $Si_{6-z}Al_zO_zN_{8-z}$ was obtained from the equations $a = 7{\cdot}603 + 2{\cdot}970 \times 10^{-2} z$ and $c = 2{\cdot}907 + 2{\cdot}55 \times 10^{-2}\ z$ Å.[5] In the quantitative estimation of the amounts of crystalline phases, the integrated intensities of the following reflections were used: (102) and (210) of the α sialon, (101) and (210) of the β sialon, (211) of the Nd-melilite and (102) of the so-called *h*-phase, an α-wollastonite-type phase of composition Y_2SiAlO_5N, which crystallizes from the intergranular glass. The corrected relative weight fraction of each phase was then calculated from the expression

$$w_k = (I_k/K_k)/\sum_{i=1}^{n} (I_i/K_i) \qquad 1 \le k \le n$$

where w_k is the weight fraction of phase k, n is the number of crystalline phases present and K_i is a constant for the intensity I_i of the selected reflection (hkl) of phase i. The K_i constants were calculated theoretically from knowledge of the structures of the phases, according to a procedure outlined in Ref. 6.

After application of a gold coating, polished surfaces of as-sintered materials were also studied in a scanning electron microscope (JEOL JSM 820, equipped with a Link AN 10 000 EDS analyzer). For some of the samples (3, 5 and 6), attempts were made to estimate the amount of intergranular phase. This was done by counting the number of bright spots on the scanning electron micrographs of the samples, using a transparent sheet of graph paper.

3 Results

3.1 Densification

The observed densities from the sintering runs at 1775 and 1825°C are summarized in Table 1. It can be seen that the samples formed at the higher temperature in general have densified better, but to obtain a stricter judgement the observed values have been transformed into percentages of the theoretical densities (% TD). To obtain a reference material for

Table 1. Observed densities at two sintering temperatures, 1 775 and 1 825 C

Sample no.	*Y_2O_3/Nd_2O_3 ratio*	*1 775 C*		*1 825 C*	
		Observed	*%TD*	*Observed*	*%TD*
1	100/0	3·195	98·6	3·231	99·7
	50/50	3·200	97·5	3·256	99·4
	0/100	3·205	96·5	3·283	99·1
2	100/0	3·234	99·8	3·246	100·0
	50/50	3·266	99·7	3·289	100·0
	0/100	3·150	94·8	3·292	99·5
3	100/0	3·244	100·0	3·242	100·0
	75/25	3·253	99·9	3·258	100·0
	50/50	3·270	99·8	3·280	100·0
	25/75	3·230	97·9	3·290	99·9
	0/100	3·194	96·4	3·310	100·0
4	100/0	3·234	99·8	3·245	100·0
	50/50	3·236	98·7	3·293	100·0
	0/100	3·173	95·4	3·270	98·8
5	100/0	3·244	100·0	3·250	100·0
	50/50	3·281	100·0	3·281	100·0
	0/100	3·302	99·7	3·316	100·0
6	100/0	3·188	98·3	3·224	99·5
	50/50	3·198	97·2	3·245	99·0
	0/100	3·075	92·3	3·260	98·2

The densities have been transformed into percentages of the theoretical density (%TD). The error in the %TD values is estimated to be ±0·5 and in the densities ±0·002 g/cm^3.

the theoretical densities, the same compositions that have been used in this work have also been sintered by glass-encapsulated hot isostatic pressing at temperatures of 1550–1825°C.[7] This procedure shows that nearly all the specimens are dense at 1825°C, including the neodymia-rich ones, which is not the case at 1775°C.

3.2 XRD phase analysis

Guinier–Hägg photographs were used for identification of the crystalline phases and determination of their cell parameters. The results are summarized in Table 2. Three tendencies can be observed. First, in the mixed α–β sialons the amount of α phase clearly decreases and the relative amount of β phase consequently increases, when yttria is replaced by neodymia. Second, for some of the samples the z-values of the β sialons seem to decrease slightly when going from a pure yttria to a pure neodymia additive. The shifts are generally small, however, and for samples 1, 2 and 5 they are scarcely significant. No corresponding shifts of the cell parameters were observed for the α sialon. Thus all samples containing the latter phase had almost the same lattice parameters centered around the values $a = 7{\cdot}80$ Å and $c = 5{\cdot}68$ Å, irrespective of phase composition and sintering temperature. Third, the Nd-melilite phase always appeared in the compositions with the highest neodymia content. Sample 3 had the largest amount of melilite and sample 4 the smallest, as might be expected from the phase diagram in Fig. 1b. The lattice parameters of the tetragonal melilite phase showed only small shifts, and were centered around 7·77 and 5·06 Å for the a- and c-axis, respectively. It can be noted that no Y-melilite was observed in any of these samples. This is in agreement with the observation that the melilite phase has an extended homogeneity range in the Nd-sialon system, whereas in the Y-sialon system melilite is believed to have a very narrow range, if any.

A more careful quantitative estimation of the decreasing amount of α-phase in a mixed α–β sialon was attempted on sample 3, using X-ray powder diffractometer data. The results are given in Fig. 3. All five Y/Nd compositions (100/0, 75/25, 50/50, 25/75 and 0/100) were measured, and it can be seen that the relative weight fraction of α sialon decreases from about 35 to 12% as the composition is changed. From the Y/Nd = 75/25 specimen to the

Table 2. Observed crystalline phases at the two sintering temperatures

Sample no.	Y_2O_3/Nd_2O_3 *ratio*	*1775°C*			*1825°C*		
		Intergranular phases[a]	$\alpha/(\alpha+\beta)$ (%)	z[b]	*Intergranular phases*[a]	$\alpha/(\alpha+\beta)$ (%)	z[b]
1	100/0	—	—	0·50	—	—	0·47
	50/50	M weak	—	0·47	M weak	—	0·49
	0/100	M	—	0·45	M	—	0·45
2	100/0	—	15	0·53	—	16	0·51
	50/50	[c]	[c]	[c]	—	15	0·50
	0/100	M	weak	0·47	M	weak	0·54
3	100/0	—	25	0·64	B[d]	[d]	0·63
	72/25	—	22	0·56	B weak	[d]	0·58
	50/50	—	17	0·56	—	[d]	0·63
	25/75	M	6	0·54	M	[d]	0·58
	0/100	M	weak	0·47	M	[d]	0·54
4	100/0	—	41	0·66	—	44	0·69
	50/50	M weak	39	0·54	—	28	0·54
	0/100	M	13	0·49	M	weak	0·56
5	100/0	—	—	0·67	B weak	—	0·66
	50/50	—	—	0·60	—	—	0·67
	0/100	M	—	0·54	M	—	0·65
6	100/0	—	58	0·41	B?	58	0·54
	50/50	M weak	48	0·47	—	55	0·52
	0/100	M	weak	0·41	M	33	0·44

[a] M = Nd-melilite, B = b-Phase.
[b] z Value of the β sialon phase, defined by $Si_{6-z}Al_zO_zN_{8-z}$.
[c] This sample was not prepared.
[d] See Fig. 3 for a more accurate estimation.

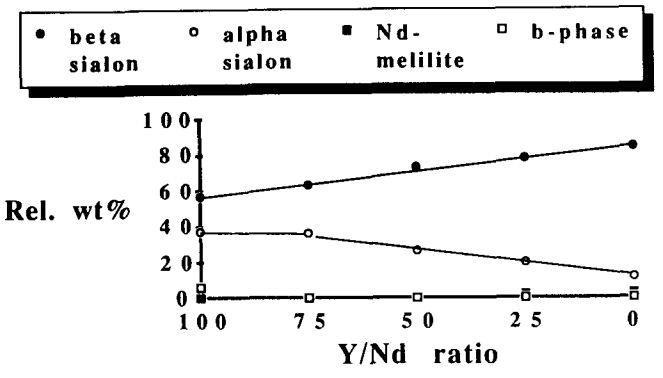

Fig. 3. The relative weight fractions of the crystalline phases in a mixed α–β sialon (sample 3) when going from 100% yttria to 100% neodymia as sintering additive. The apparent increase in the relative weight fractions of β sialon is not established on an absolute scale but rather is a reflection of the decreasing amount of α sialon and the increasing amount of intergranular phase. ●, β-sialon; ○, α-sialon; ■, Nd-melilite; □, *h* phase.

0/100 one the decrease is practically linear. At the same time, the relative amount of β phase increases from less than 60 to ~85%. However, examination of scanning electron micrographs (see below) revealed that this increase was probably not significant on an absolute scale, but was merely a consequence of the simultaneous decrease in the α sialon content and the increasing amount of intergranular phase.

The calculated weight fraction of Nd-melilite was 2% in the 25/75 sample, and 3% in the 0/100 sample. It can be noted that these values are substantially lower (about six times) than those that would be obtained from simple peak-height measurements, where no corrections are made for the varying scattering power for X-rays of the different phases. In the pure yttria specimen 6% *h*-phase was observed. Traces of this phase were also present in the 75/25 composition but were too weak to be estimated quantitatively.

3.3 Microstructure

Scanning electron micrographs of the samples 3, 5 and 6, sintered at 1825°C, are shown in Figs 4(a)–(c), 5(a)–(c) and 6(a)–(c) (backscattered electron mode). Sample 5 (Fig. 4(a)–(c)) is a β sialon, although small amounts of *h*-phase were observed in the sample sintered with pure yttria, and, similarly, small amounts of melilite were seen in the pure neodymia sample. No really significant change of the aspect ratios or the sizes of the β sialon grains (dark grey) seems to take place in sample 5, when yttria is replaced by neodymia. On the other hand, it is clear that the amount of intergranular phase increases as the neodymia content increases. The increase of the intergranular phase (bright areas) is of the order ~8

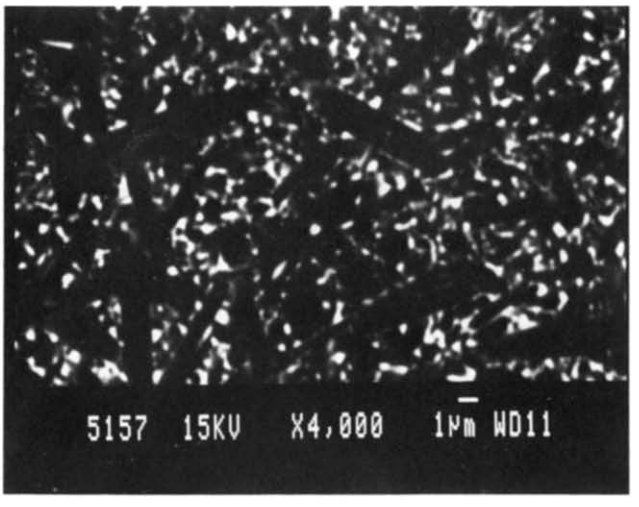

(a)

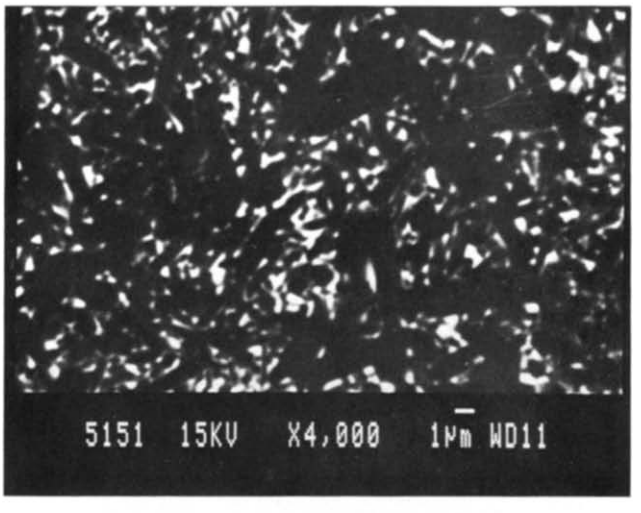

(b)

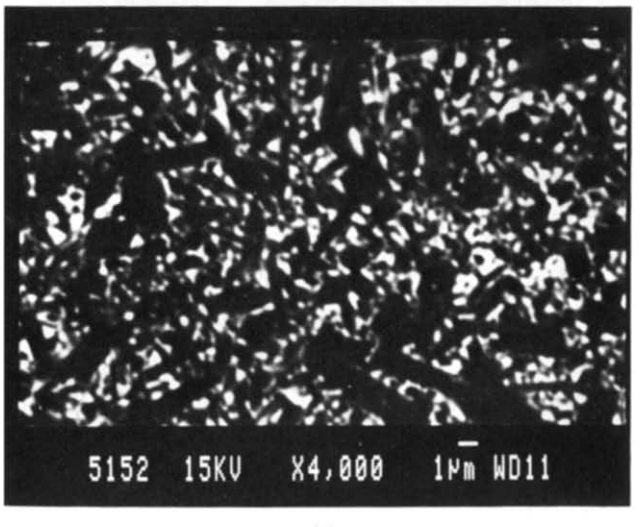

(c)

Fig. 4. Scanning electron micrographs (backscattering mode) of a β sialon material (sample 5). The sample was sintered pressurelessly at 1825°C. The sintering additives are varied in the following way: (a) 100% Y_2O_3, (b) 50/50 Y_2O_3–Nd_2O_3, (c) 100% Nd_2O_3.

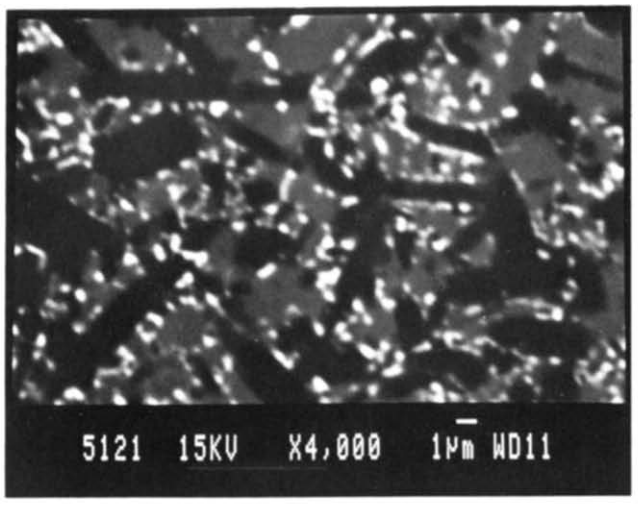

(a)

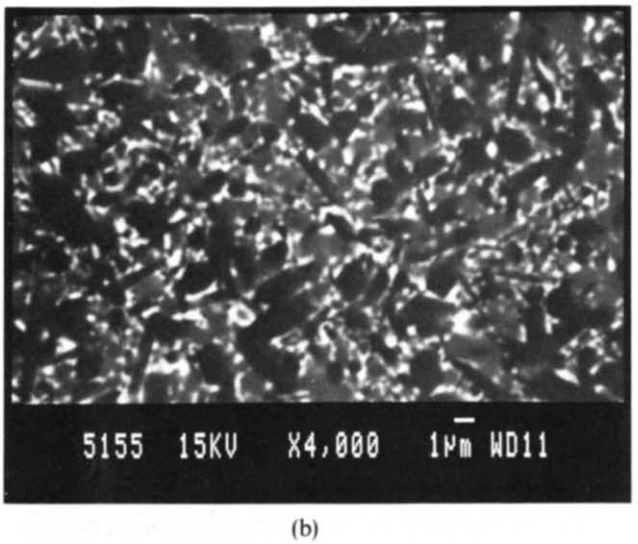

(b)

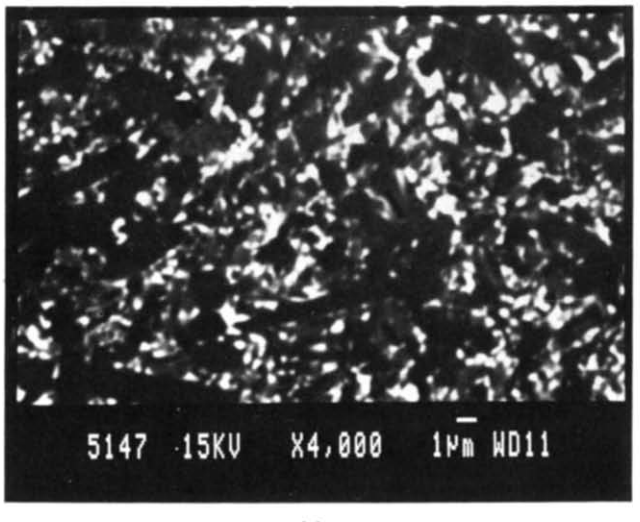

(c)

Fig. 5. Scanning electron micrographs of a mixed α–β sialon (sample 3) sintered pressurelessly at 1825°C. The sintering additives are varied as in Fig. 4(a)–(c). The dark grains are the β sialons, the medium grey areas the α sialons and the bright areas the intergranular phase. The decrease in the α sialon content is clearly seen in this series, as is the increase in the amount of intergranular phase.

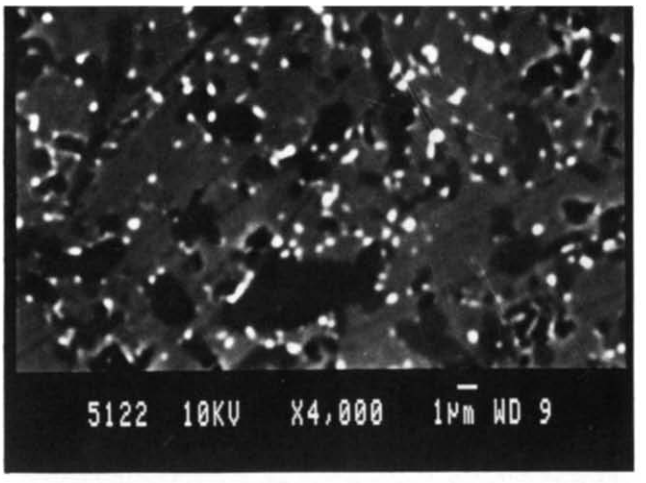

(a)

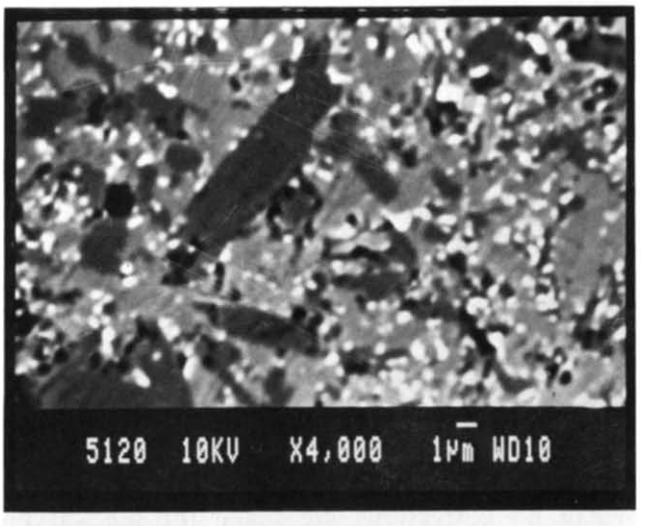

(b)

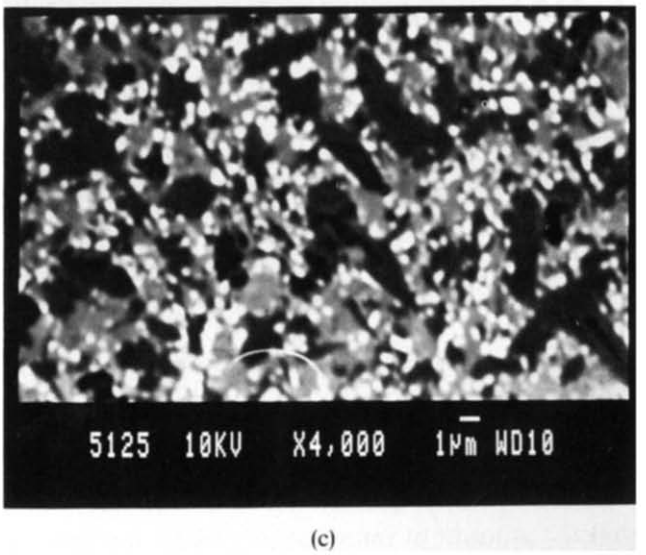

(c)

Fig. 6. Scanning electron micrographs of sample 6, a mixed α–β sialon. See also caption for Fig. 5(a)–(c).

to ~20 vol%. (We found very similar results for sample 1, another β sialon, when it was sintered at 1775°C.[3])

The changes of the mixed α–β sialon samples 3 and 6, sintered at 1825°C, are seen in Fig. 5(a)–(c) and Fig. 6(a)–(c). At least three types of changes can be observed:

(1) The size of the β sialon grains (dark grey) diminishes and they become more needle-like. These changes are accompanied by a shift in the z-value from ~0·63 to ~0·54 in sample 3 and from ~0·54 to ~0·44 in sample 6. For sample 5, where no changes of the β sialon grains can be seen, no shifts of the z-value were observed either.

(2) The α-sialon content (medium grey areas) decreases.

(3) The amount of intergranular phase increases. The estimated increase in the intergranular phase in both of these samples is from ~6 to ~16 vol%.

It has been suggested above that the relative increase in the amount of β phase in a mixed α–β sialon, as shown in Fig. 3, seems to be a result of the reduction of the α sialon content and not an increase in the absolute amount. This is confirmed by the fact that the two changes observed when yttria is replaced by neodymia are the decreasing amount of α sialon and the increasing amount of intergranular phase.

3.4 EDS analysis

To obtain the best quantitative data possible in the energy dispersive spectrometry (EDS) analysis, a calibration curve of the Al/Si signals was prepared, using as references a series of β sialon samples with accurately known contents of Al and Si.

It was not possible to distinguish the glass from the crystalline Nd-melilite in the scanning electron microscope, but the EDS technique clearly indicated the presence of two different species in the intergranular areas. In the overall microstructure four phases could be distinguished from the ZAF-corrected Nd-signals in the 0/100 composition of sample 6. The relative magnitudes of these signals, expressed as atomic percentages, were of the order ~0, 2·9 ± 0·7, 7·4 ± 0·6, 12·3 ± 1·2, corresponding to β sialon, α sialon and glass/Nd-melilite, respectively. The strongest signal probably comes from the melilite, a phase that is assumed to contain almost 17 at% of Nd. The composition of the α sialon of sample 6 was found by EDS analysis to be

$$Y_{0\cdot40\pm0\cdot05}Si_{10\cdot4\pm0\cdot1}Al_{1\cdot6\pm0\cdot1}O_{0\cdot4\pm0\cdot2}N_{15\cdot6\pm0\cdot2}$$

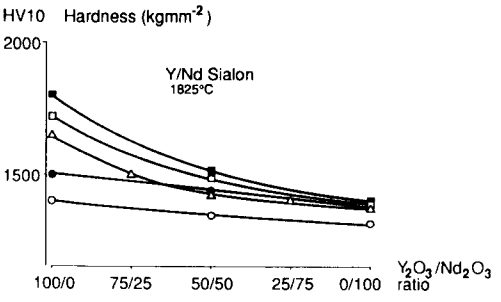

Fig. 7. The variation in measured Vickers hardness (load 98 N, HV10 scale) when yttria is gradually replaced by neodymia as sintering additive in pressureless sintering at 1825 C. The estimated accuracy in the HV10 values is ±30 units. ○, No. 1; △, 2; □, 3; ●, 4; ■, 5.

in the pure yttria specimen and

$$Nd_{0\cdot33\pm0\cdot01}Si_{10\cdot5\pm0\cdot1}Al_{1\cdot5\pm0\cdot1}O_{0\cdot5\pm0\cdot1}N_{15\cdot5\pm0\cdot1}$$

in the pure neodymia specimen.

3.5 Physical properties

The results of the hardness (HV10) and indentation fracture toughness (K_{IC}) measurements are represented in Figs 7 and 8. At 1825°C a slight drop in hardness is observed for most compositions when moving from 100% yttria to 100% neodymia. The fracture toughness, however, remained essentially of the same magnitude, irrespective of the additive used. The decrease in hardness may originate from two sources: the increasing amount of 'soft' intergranular phase in all compositions and, in the mixed α–β sialons, the decreasing relative amount of the α sialon phase, which is harder than the β sialon.

4 Discussion

At 1775°C it is clearly illustrated (Table 1) how the replacement of Y_2O_3 by Nd_2O_3 diminishes the effect of the sintering process in most samples. Only the sample 5 compositions have acceptable densities regardless of the sintering aid used. This might be expected, as these compositions contain most

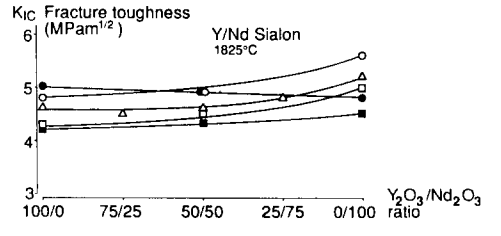

Fig. 8. The variation in measured indentation fracture toughness (K_{IC}) when yttria is gradually replaced by neodymia as sintering additve in pressureless sintering at 1825°C. The estimated accuracy in the K_{IC} values is ±0·2 MPa $m^{1/2}$. ○, No. 1; △, 2; □, 3; ●, 4; ■, 5.

oxygen and a considerable amount of aluminium as well, both acting as fluxing agents. On the other hand, sample 1, which has a low aluminium content, and sample 6, which is low in oxygen, both consolidated slowly even when pure yttria additive was used at the lower temperature.

At 1825°C nearly all samples sintered to a density $\geq 99\%$ TD, the only exception being the 0/100 composition of sample 6. It can therefore be said that at this higher temperature pressureless sintering of Nd-sialon ceramics is well achieved.

The α sialon phase observed in this study has unit cell dimensions of about $a = 7{\cdot}80$ Å and $c = 5{\cdot}68$ Å, regardless of the overall composition or the added Y_2O_3/Nd_2O_3 ratio. By EDS analysis we have obtained $x = 0{\cdot}40 \pm 0{\cdot}05$ for Y and $x = 0{\cdot}33 \pm 0{\cdot}01$ for Nd in $M_x(Si, Al)_{12}(O, N)_{16}$. The estimated error in the x-value is somewhat bigger for Y than for Nd, because of the strong overlap between the Si K and the Y L X-ray emission lines. These data are in good agreement with those given by Stutz *et al.*,[8] who found the same lattice parameters for the lowest concentration of Y ($x = 0{\cdot}33$) in α sialon. In fact, they showed that the unit cell is larger for all other compositions within the two-dimensional solid solution area of yttrium α sialon. Our results also agree well with Huang *et al.*,[9] who found that the lower limit of x is $\sim 0{\cdot}33$ for all rare earth cations which can be accepted by the α sialon lattice, corresponding to the cell parameters $a = 7{\cdot}80$ Å and $c = 5{\cdot}69$ Å.

It is a notable fact that the variation of the composition of the α-phase is very small in this study; it seems to be insensitive to the overall starting composition of the α–β samples. This phenomenon can be explained, at least qualitatively, in the following way. The selected α–β compositions (Fig. 2) all lie rather close to the N-rich corner of the solid solution area of the α-phase. Moreover, because of the sintering additive, each α–β sample will be in 'equilibrium' not only with the α- and β-phases but also with an intergranular phase (i.e. glass and/or melilite). As the latter phase(s) will consume both some of the heavy elements (Y, Nd) and some of the lighter ones (O, Al), we should expect a drift towards the N-rich endpoints of the resulting α- and β-phases, and this is also observed. It might well be correct to say that the selected α–β compositions in this study are in 'equilibrium' not with the α-phase area as a whole but rather with a small subarea close to the lower end of the substitution range.

It has already been mentioned that the most commonly observed crystalline phase, besides the α and β sialons, is the Nd-melilite. This compound has an extended homogeneity range in the three-dimensional Nd-sialon phase diagram (Fig. 1b). The Nd-melilite, $Nd_2Si_{3-x}Al_xO_{3+x}N_{4-x}$, has a tetragonal lattice and a seemingly linear expansion of the cell parameters from $a = 7{\cdot}718$ Å, $c = 5{\cdot}031$ Å to $a = 7{\cdot}765$ Å, $c = 5{\cdot}045$ Å in the interval $0 \leq x \leq 0{\cdot}9$.[10] From the lattice parameters observed in this study we therefore conclude that the melilite phase has a composition of about $Nd_2Si_{2{\cdot}1}Al_{0{\cdot}9}O_{3{\cdot}9}N_{3{\cdot}1}$, i.e. very close to the highest possible substitution of Al for Si.

5 Conclusions

The following conclusions can be drawn:

(1) At 1825°C a fully dense sialon material can be sintered pressurelessly where yttria has been replaced by neodymia as sintering additive.

(2) The Vickers hardness (HV10) of Nd-sialons is slightly lower than for the corresponding Y-sialons, but the fracture toughness (K_{IC}) is approximately of the same magnitude.

(3) It seems impossible to achieve the same high α/β ratio in mixed α–β sialons when neodymia is used instead of yttria as sintering aid for the same overall composition.

(4) Nd-sialons contain larger volumes of intergranular phase than do the corresponding Y-sialons.

(5) In the mixed α–β samples the resulting α-phase is found to have the same chemical composition, corresponding to a point close to the lower end of the substitution range.

Acknowledgements

The authors are grateful to Dr Kath Liddell at the Department of Metallurgy and Engineering Materials, Newcastle upon Tyne, UK, for her kind help in heat-treating some of our samples. Dr Mats Nygren at the Arrhenius Laboratory is thanked for his stimulating interest in and comments on this manuscript. The work has been financed in part by the Swedish Board for Technical Development and in part by AB Sandvik Hard Materials in Stockholm.

References

1. Park, H. K., Thompson, D. P. & Jack, K. H., α'-SIALON ceramics. *Sci. Ceram.*, **10** (1980) 251.
2. Slasor, S., Liddell, K. & Thompson, D. P., The role of Nd_2O_3

as an additive in the formation of α' and β' sialons. *Br. Ceram. Proc.*, **37** (1986) 51.
3. Ekström, T., Käll, P-O., Nygren, M. & Olsson, P-O., Mixed α- and β-(Si–Al–O–N) materials with yttria and neodymia additions. *Mater. Sci. Eng.*, **A105/106** (1988) 161.
4. Anstis, G. R., Chantikul, P., Lawn, B. R. & Marshall, D. P., A critical evaluation of indentation techniques for measuring fracture toughness: I, direct crack measurements. *J. Am. Ceram. Soc.*, **64** (1981) 533.
5. Ekström, T., Käll, P-O., Nygren, M. & Olsson, P.-O., Dense single-phase β-sialon ceramics by glass-encapsulated hot isostatic pressing. *J. Mater. Sci.*, **24** (1989) 1853.
6. Käll, P-O., Quantitative phase analysis of Si_3N_4-based materials. *Chem. Scripta*, **28** (1988) 439.
7. Käll, P-O. & Ekström, T., Phase composition and mechanical properties of HIP-sintered Y/ND-sialon ceramics. To be presented at the 11th Risø International Symposium on Metallurgy and Materials Science, August 1990.
8. Stutz, D., Greil, P. & Petzow, G., Two-dimensional solid-solution formation of Y-containing α-Si_3N_4. *J. Mater. Sci. Lett.*, **5** (1986) 335.
9. Huang, Z. K., Tien, T. Y. & Yen, T. S., Subsolidus phase relationships in the Si_3N_4–AlN–Rare-Earth Oxide Systems. *J. Am. Ceram. Soc.*, **69** (1986) C-241.
10. Käll, P-O., Homogeneity range and oxidation behaviour of the melilite phase present in some sialon systems. To be published.